Li$_3$PO$_4$-added garnet-type Li$_{6.5}$La$_3$Zr$_{1.5}$Ta$_{0.5}$O$_{12}$ for Li-dendrite suppression

CrossMark

Biyi Xu [a, 1], Wenlong Li [b, c, 1], Huanan Duan [a, *], Haojing Wang [b, c], Yiping Guo [a], Hua Li [a], Hezhou Liu [a, **]

[a] State Key Laboratory of Metal Matrix Composites, School of Materials Science and Engineering, Shanghai Jiao Tong University, Shanghai, 200240, PR China
[b] State Key Laboratory of Transient Optics and Photonics, Xi'an Institute of Optics and Precision Mechanics, Chinese Academy of Sciences, Xi'an, Shaanxi, 710119, PR China
[c] University of Chinese Academy of Sciences, Beijing, 100049, PR China

HIGHLIGHTS

- Li$_3$PO$_4$-Li$_{6.5}$La$_3$Zr$_{1.5}$Ta$_{0.5}$O$_{12}$ (LPO-LLZT) is prepared by solid−state reaction.
- The ionic conductivity of LPO-LLZT at 25 °C is 1.4×10^{-4} S cm^{-1}.
- LPO decreases the LLZT/Li interfacial resistance from 2080 Ω cm^2 to 1008 Ω cm^2.
- Symmetric cells with LPO-LLZT are cycled at 0.1 mA cm^{-2} and 60 °C for 60 h.
- The interface stability results from the *in situ* formed Li$_3$P near grain boundaries.

GRAPHICAL ABSTRACT
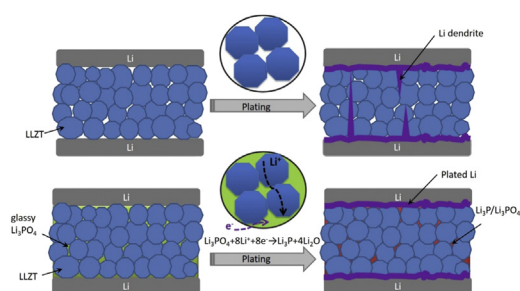
ARTICLE INFO

ABSTRACT

This paper proposes a strategy to stabilize the garnet/Li interface by introducing Li$_3$PO$_4$ as an additive in garnet-type Li$_{6.5}$La$_3$Zr$_{1.5}$Ta$_{0.5}$O$_{12}$. The Li$_3$PO$_4$-added Li$_{6.5}$La$_3$Zr$_{1.5}$Ta$_{0.5}$O$_{12}$ electrolyte exhibits a room-temperature Li-ion conductivity of 1.4×10^{-4} S cm^{-1}, which is less than that of the Li$_3$PO$_4$-free counterparts (4.6×10^{-4} S cm^{-1}). However, the presence of Li$_3$PO$_4$ improves the interfacial compatibility and suppresses Li-dendrite formation during Li-metal plating/stripping. The symmetric Li/garnet/Li cells with Li$_3$PO$_4$-added Li$_{6.5}$La$_3$Zr$_{1.5}$Ta$_{0.5}$O$_{12}$ have been successfully cycled at a current density of 0.1 mA cm^{-2} at 60 °C for 60 h; on contrast, the control cells with Li$_3$PO$_4$-free Li$_{6.5}$La$_3$Zr$_{1.5}$Ta$_{0.5}$O$_{12}$ display noisy potential with large voltage polarization and get short-circuited completely after 33-h cycling under the same operating condition. The outstanding interface stability can be attributed to the *in situ* reaction of the Li flux with Li$_3$PO$_4$ to form a self-limiting and ion-conducting interphase, Li$_3$P, which is confirmed experimentally.

© 2017 Elsevier B.V. All rights reserved.

1. Introduction

Li metal with a high theoretical specific capacity (3860 mA h g^{-1}) and a low electrochemical potential (-3.04 V vs. H$^+$/H^0) has been pursued for decades as an anode in Li-ion batteries

---

(LIBs) [1]. More recently, it has been regarded as one of the key materials to take the full advantage of the post-LIB devices such as Li/air, Li-S, and all solid-state Lithium batteries. However, the application of Li metal is significantly restricted by its inherent reactivity with conventional organic liquid electrolytes, as well as the formation and propagation of lithium dendrites during cycling, which usually leads to low Coulombic efficiency of the batteries [2], short circuit, even catastrophic failure [3,4]. At present, developing lithium batteries simultaneously possessing high safety, excellent reversible capacity, and low cost still remains an enormous challenge.

In traditional LIBs, organic electrolytes react with Li metal and form a solid electrolyte interphase (SEI) layer on the Li surface. During the charging of LIBs, the SEI layer is easy to be broken as a result of the Li deposition; this will expose fresh Li metal to the liquid electrolyte and generate more SEI layers. At the same time, the broken SEI layer will cause local non-uniformity of current density and electron and/or lithium ion concentration, which will lead to preferential deposition of Li metal locally and subsequently Li-dendrite growth. Eventually, the growing lithium dendrites may pierce through the polymer separator to make the batteries short-circuited. To suppress the formation of Li dendrites, various strategies have been tried out, including functional additives [5], artificial SEI layer [6], ultra-strong separators [7], nanostructured anodes [8], and electrodes alloying [9]. However, these strategies have only achieved limited success because they do not change the thermodynamic tendency for Li metal to react with organic electrolyte.

Another possible solution to protect Li against dendrite penetration is to develop inorganic solid electrolytes because of their unity Li ion transference number, chemical inertness, and high mechanical strength [10]. Recently, garnet-type $Li_7La_3Zr_2O_{12}$ has attracted much attention because of its compatibility with Li metal and high Li-ion conductivity (4×10^{-4} S cm^{-1}) at room temperature [11–17]. However, garnet electrolyte can not suppress the Li-dendrite formation, and a 'short circuit' phenomenon has been observed in a symmetric Li/garnet-based electrolyte/Li cell even at a small current density [18]. It was speculated that this phenomenon was attributed to the lithium dendrite growth through the grain boundaries and voids inside the electrolyte [19]. Moreover, various factors have been argued to be able to directly affect the short-circuit period such as the relative elasticity modulus of the electrolyte [20], the lithium ion diffusion kinetics at the grain boundaries [21], and the impurity phase (i.e. Li_2CO_3) formed on the sample surface exposed to air [22,23]. Recently, an interesting strategy that engineered the LLZO surface to be porous was proposed to enhance Li$^+$ transfer and decrease the interface resistance of the garnet/$Li_4Ti_5O_{12}$ interface, however the effect of Li dendrite suppression is not clear [6]. Another approach that has attracted much attention is to deposit a thin coating on the LLZO surface to reduce the interfacial resistance, and various materials including Au, Nb, Si and Al_2O_3 have been tried out; however, the coating breaks down beyond the limiting current density [24–26]. Till now, a rational design to stabilize the garnet electrolyte/lithium metal interface remains missing, especially at a high current density and for a prolonged cycling test.

Inspired by the self-limiting passivation layer formed at the $LiZr_2(PO_4)_3$/Li interface [27], in this work, we propose an alternative strategy to stabilize the garnet/Li interface by introducing Li_3PO_4 as a second phase additive for the garnet electrolyte. The results show that glassy Li_3PO_4 phase is distributed on the garnet grain boundaries. The symmetric cell with Li_3PO_4-added garnet has been cycled galvanostatically for over 60 h at 60 °C; on contrast, the symmetric cell with a Li_3PO_4-free garnet exhibits complete short-circuit after around 33 h cycling. Based on spectroscopy study, it is speculated that the Li_3PO_4 additive can *in situ* react with the plated Li to form Li_3P during charge processes, which effectively stabilizes the garnet/Li interface and suppresses the lithium dendrite propagation.

2. Experimental and characterization

All the reagents—unless otherwise noted—were purchased from Sinopharm Chemical Reagent Co., Ltd. Briefly, proper amount of Li_2CO_3 (99.99%, with 10% excess to compensate the sintering loss), La_2O_3 (99.95%), ZrO_2 (99.97%), Ta_2O_5 (99.99%) were ground in a mortar to obtain stoichiometry of $Li_{6.5}La_3Zr_{1.5}Ta_{0.5}O_{12}$ (designated as LLZT). The mixture was calcined at 900 °C for 6 h, then the obtained mother powders were reground with 5 wt% Li_3PO_4 (99.99%) for another 1 h and pressed into pellets with a diameter of 10 mm (designated as LLZT-LPO). The green pellets were buried by the mother powder and sintered in aluminum crucibles with a cover at 1140 °C for 16 h. The resulting pellets were polished with P2000 sand paper and stored in an Ar-filled glovebox (<0.1 ppm O$_2$, <0.1 ppm H$_2$O) to prevent reaction with humidity.

The structural characterization was performed by X-ray diffraction (XRD, D/MAX255ovl/84, Rigaku, Japan) with 2θ in the range of 10−60° with a step size of 0.02°. The ionic conductivity was calculated from data collected by an impedance analyzer (Solartron 1260) in the frequency range from 10 MHz to 1 Hz with 10 mV amplitude at room temperature. A symmetric cell was assembled by stacking lithium garnets between two Li foils (Aladdin) in a Swagelok cell, and a spring was added to improve the contact between the garnets and Li foils. The cells were left in an oven overnight at 60 °C before cycling tests. The resistance values of garnet/Li interface were calculated based on dividing experimental resistance by two, and then normalizing to the contact interface area. The lithium plating/stripping test was carried out by galvanostatic cycling with a LAND CT2001A cell test system at a fixed current density at 60 °C. Morphology study was performed before and after cycling tests using a scanning electron microscopy (SEM, TM 3000 tabletop microscope, Hitachi) equipped with Energy-dispersive X-ray spectra (EDS). X-ray photoelectron spectroscopy (XPS, AXIS Ultra DLD, Kratos, Japan) was employed to collect surface chemistry information of the garnet samples before and after cycling.

3. Results and discussion

SEM images of LLZT and LLZT-LPO are depicted in Fig. 1a–b. Clearly, both LLZT and LLZT-LPO are well densified; there is a small amount of intergranular glassy phase near the grain boundaries of LLZT-LPO. The EDS mapping (Fig. 1c) indicates that for LLZT-LPO, the element of P is concentrated near the grain boundaries. XRD patterns of LLZ and LLZ-LPO are shown in Fig. 1d. All peaks can be assigned to the cubic garnet phase (PDF #45-0109); no peaks of Li_3PO_4 were detected for the LLZT-LPO samples. As reported in our previous work, tetragonal garnet forms partially after the first sintering step at 900 °C, and the second sintering step at higher temperature (i.e. 1140 °C) leads to a phase transformation from tetragonal to cubic garnet and densification [15]. Here when Li_3PO_4 is introduced in the second sintering step, it tends to melt and form amorphous phase near the grain boundaries since the temperature of 1140 °C is higher than the melting point of the Li_3PO_4 (837 °C) [28].

The Nyquist plots of LLZT and LLZT-LPO, as shown in Fig. 1e, are used to evaluate the Li-ion conductivity. The impedance plots consist of one suppressed semicircle and a tail, which can be fitted with the equivalent circuit shown in the inset. The room-temperature Li-ion conductivities of LLZT and LLZT-LPO are